bioRxiv preprint doi: https://doi.org/10.1101/2022.11.27.518067; this version posted November 27, 2022. The copyright holder for this preprint (which was not certified by peer review) is the author/funder, who has granted bioRxiv a license to display the preprint in perpetuity. It is made available under aCC-BY-NC 4.0 International license.

Multiple rod layers increase the speed and sensitivity of vision in nocturnal reef fishes

Lily G. Fogg[1*], Wen-Sung Chung[1], Fabio Cortesi[1], N. Justin Marshall[1], Fanny de Busserolles[1]

[1]Queensland Brain Institute, The University of Queensland, Brisbane, Queensland, 4072, Australia

*Corresponding author email: lily.fogg@uqconnect.edu.au

bioRxiv preprint doi: https://doi.org/10.1101/2022.11.27.518067; this version posted November 27, 2022. The copyright holder for this preprint (which was not certified by peer review) is the author/funder, who has granted bioRxiv a license to display the preprint in perpetuity. It is made available under aCC-BY-NC 4.0 International license.

1 **Abstract**
2 Multibank retinas have rod photoreceptors stacked into multiple layers. They are found in many
3 species of fish that inhabit dim environments and are one of the most common visual adaptations in
4 the deep-sea. Despite its prevalence, the function of multibank retinas remained unknown. Two
5 predominant theories, neither of which has been tested, have emerged: 1) they enhance sensitivity in
6 dim light, and 2) they allow colour vision in dim light. To investigate the sensitivity hypothesis, we
7 performed electrophysiological recordings and compared the rod pigments of three species of
8 nocturnal reef fishes, two with a multibank retina (*Neoniphon sammara* and *Myripristis violacea*) and a
9 control species with a single rod bank (*Ostorhinchus compressus*). Results indicated that nocturnal
10 reef fishes with a multibank retina have higher temporal resolution of vision, as indicated by
11 electrophysiology, and that their rhodopsin proteins likely also have faster retinal release kinetics, as
12 suggested by amino acid substitutions. Electrophysiology also showed that the multibank retina
13 conferred greater sensitivity to both dim and bright intensities than a single rod bank and this occurred
14 at times when rod-derived signals usually dominate the visual response. This study provides the first
15 functional evidence for enhanced dim-light sensitivity using a multibank retina while also suggesting
16 novel roles for the adaptation in enhancing bright-light sensitivity and the speed of vision.

17

Significance

18 Most vertebrates have one layer of the dim-light active rod photoreceptors; however, some species
19 have multiple layers, known as a multibank retina. We used electrophysiology on nocturnal reef fishes
20 with and without multibank retinas to evaluate the sensory advantage of having multiple rod layers.
21 We show that fish with multibank retinas have both faster vision and enhanced sensitivity to bright
22 and dim light intensities. Thus, we resolve for the first time the function of multibank retinas – one of
23 the most common visual adaptations in the deep sea. Our findings highlight an unconventional
24 vertebrate visual system as well as the visual capabilities of fishes from the most vast (deep sea) and
25 vibrant (reefs) ecosystems on the planet.

bioRxiv preprint doi: https://doi.org/10.1101/2022.11.27.518067; this version posted November 27, 2022. The copyright holder for this preprint (which was not certified by peer review) is the author/funder, who has granted bioRxiv a license to display the preprint in perpetuity. It is made available under aCC-BY-NC 4.0 International license.

26 **Introduction**

27 A great diversity of visual adaptations has evolved across the animal kingdom to permit vision in a
28 myriad of ecological niches. For example, in invertebrates, these visual adaptations range from the 12
29 colour photoreceptors of the mantis shrimp (1) to the polarisation vision of locusts used for celestial
30 navigation (2). While in terrestrial vertebrates, these adaptations include the hybrid cone-like rods of
31 colubrid snakes (3, 4) to the highly sensitive eyes of some geckos that can discriminate colour in
32 moonlight (5). Marine fishes are no exception to this diversity (6). To catch as many photons as
33 possible, marine fishes living in dim-light environments such as in the deep-sea or at night show
34 arguably the most extreme visual adaptations among vertebrates (7, 8). These scotopic adaptations
35 include enlarged eyes or tubular eye structures (9, 10), high expression of the rod opsin gene, *rh1*
36 (11, 12), high rod densities (13, 14), and thick photoreceptor layers, either through longer rods or
37 multiple layers of rods, known as a multibank retina (12, 15, 16). Although many of these adaptations
38 have been attributed to increasing sensitivity, the function of the multibank retina remained untested.

39 Multibank retinas consist of 2-28 layers of stacked rods (16, 17) and have been found in
40 representatives from at least 38 teleost fish families (7, 18), the vast majority of which are deep-sea
41 species (7). Two predominant theories have been suggested to explain their function. The first theory
42 proposes that multibank retinas enhance luminous sensitivity by increasing the cumulative rod outer
43 segment length available for photon capture (19). The second theory suggests that they allow colour
44 vision in dim light through spectral filtering at each layer and an opponent comparison between the
45 layers (20). Until now, few studies have examined the function of multibank retinas (21-23), due to the
46 difficulty in accessing, handling, and maintaining deep-sea fishes (16, 24). However, the recent
47 characterisation of multibank retinas in an easily accessible family of nocturnal coral reef fishes,
48 Holocentridae (12), enabled us to test the sensitivity hypothesis.

49 Holocentridae is composed of two sub-families: squirrelfishes (Holocentrinae) and
50 soldierfishes (Myripristinae). They mainly inhabit shallow depth ranges, however, a few species dwell
51 as deep as 640 metres (25, 26). Holocentrids are nocturnal (27) and as such, they have a typical dim
52 light-adapted visual system with large eyes (9), a rod-dominated retina (12, 28), a short focal length
53 (15), a high summation of rods onto ganglion cells (GC) (29) and *rh1* genes with spectral sensitivities
54 that are tuned to the dominant wavelengths at their prevalent depth (30). They also possess a highly
55 developed multibank retina, with up to 7 and 17 banks in squirrelfishes and soldierfishes, respectively
56 (12). However, holocentrids have also retained some photopic adaptations, including the potential for
57 dichromatic colour vision (12).

58 In this study, the sensitivity theory was tested by assessing the visual systems of two
59 holocentrid species (*Neoniphon sammara* and *Myripristis violacea*), and a non-multibank control
60 species (*Ostorhinchus compressus*). Firstly, retinal structure was examined using histology. Then, the
61 luminous sensitivity and temporal resolution of their vision was studied by recording the
62 electrophysiological response of the whole eye to different light stimuli, a technique known as
63 electroretinography (ERG) (31-34). Finally, we estimated the retinal release rate of the rhodopsin

bioRxiv preprint doi: https://doi.org/10.1101/2022.11.27.518067; this version posted November 27, 2022. The copyright holder for this preprint (which was not certified by peer review) is the author/funder, who has granted bioRxiv a license to display the preprint in perpetuity. It is made available under aCC-BY-NC 4.0 International license.

64 paralog expressed in the rods of each species. Overall, this study sheds light on the unresolved
65 function of a prevalent but understudied visual adaptation in the deep sea as well as offering a
66 broader insight into the vision of nocturnal reef fishes.

bioRxiv preprint doi: https://doi.org/10.1101/2022.11.27.518067; this version posted November 27, 2022. The copyright holder for this preprint (which was not certified by peer review) is the author/funder, who has granted bioRxiv a license to display the preprint in perpetuity. It is made available under aCC-BY-NC 4.0 International license.

67 **Results**

68 *Holocentrids have high rod densities and high scotopic summation*

69 Retinal architecture and cell densities were assessed in *O. compressus*, *N. sammara* and *M. violacea*
70 (*n*=1). All three species had duplex retinas composed of both rods and cones. However, while *O.*
71 *compressus* only had a single layer of rods (Fig. 1Ai, Fig. S1), *N. sammara* and *M. violacea* had a
72 maximum of 6 and 14 banks of rods, respectively (Fig. 1Aii-iii, Fig. S1). The densities of all cell types
73 were heterogeneous across the retina in all species (Fig. 1B, Table S2). In every region, the highest
74 rod densities and summation of rods onto GC occurred in *M. violacea* (peak rod densities, 21,296
75 cells/0.01mm^2; peak rod:GC ratio, 1,651.5 rods/GC) followed by *N. sammara* (peak rod, 12,403
76 cells/0.01mm^2; peak rod:GC, 332.6 rods/GC) and then *O. compressus* (peak rod, 3,545
77 cells/0.01mm^2; peak rod:GC, 78.1 rods/GC). An inverse pattern was observed for cone and GC
78 densities in all regions, with *O. compressus* having the highest densities and *M. violacea* the lowest
79 (*O. compressus*: 72.8 cells/0.01mm^2 and 97.5 cells/0.01mm^2 for peak cone and GC, respectively; *N.*
80 *sammara*: 49.4 cells/0.01mm^2 and 71.0 cells/0.01mm^2; *M. violacea*: 19.5 cells/0.01mm^2 and 29.2
81 cells/0.01mm^2). Finally, inner nuclear layer (INL) cell densities were also highest in *O. compressus*
82 and lowest in *M. violacea* for most regions (*i.e.,* dorsal, central and temporal) (peak INL, *O.*
83 *compressus*: 1108 cells/0.01mm^2; *N. sammara*: 789 cells/0.01mm^2; *M. violacea*: 638 cells/0.01mm^2).

84

85 *Holocentrids have a higher temporal resolution compared to cardinalfish*

86 Temporal resolution ERGs were conducted to determine the flicker fusion frequency (FFF; the point at
87 which evenly spaced light pulses can no longer be distinguished as separate) in response to dim (4
88 lux) and bright (384 lux) stimuli at day (*n*=3) and night (*n*=5) (Fig. S2). Under all conditions, *N.*
89 *sammara* attained the greatest FFF [mean ± s.e.m. at day and night, respectively: dim: 50±7.6 Hz and
90 33±3.7 Hz; bright: 70±2.9 Hz and 42.5±2.5 Hz; $p<0.05$ except for dim stimuli during the day which
91 was not significant (n.s.)], followed by *M. violacea* (dim: 43.3±1.7 Hz and 20±0 Hz; bright: 57.5±2.5 Hz
92 and 25±0 Hz) and then *O. compressus* (dim: 38.3±1.7 Hz and 17±2.5 Hz; bright: 41.7±1.7 Hz and
93 13±4.9 Hz) (Fig. 2; Fig. S3; Table S3). Furthermore, holocentrids had lower FFFs when exposed to
94 the dim stimulus compared to the bright stimulus at each time point ($p<0.05$ for dim vs. bright stimulus
95 during the day and dim vs. bright stimulus at night for both species; Table S3). However, the FFFs of
96 *O. compressus* did not vary greatly with stimulus intensity. Finally, all species showed a trend towards
97 lower FFFs at night compared to during the day, irrespective of stimulus intensity ($p<0.0001$ for day
98 vs. night for bright stimulus and day vs. night for dim stimulus for all species; Table S3).

99

100 *Holocentrids have enhanced sensitivity compared to cardinalfish to both bright and dim light at night*

101 Absolute sensitivity ERGs were recorded for *O. compressus* (*n*=5), *N. sammara* (*n*=4 and 5 for day
102 and night recordings, respectively), and *M. violacea* (*n*=4) during the day and night (Fig. S2; Fig. S4).

bioRxiv preprint doi: https://doi.org/10.1101/2022.11.27.518067; this version posted November 27, 2022. The copyright holder for this preprint (which was not certified by peer review) is the author/funder, who has granted bioRxiv a license to display the preprint in perpetuity. It is made available under aCC-BY-NC 4.0 International license.

103 Firstly, *V/logI* curves were normalised to either V_{max} alone (for sensitivity of the entire eye; Fig. 3A) or
104 V_{max} and eye size (for sensitivity per unit of retina; Fig. 3B). In all species, *V/logI* curves produced
105 non-monotonic functions, with the amplitude of the b-wave representing the response post-synaptic to
106 the photoreceptor, generally increasing with stimulus intensity until the maximal amplitude (V_{max}) was
107 reached, before subsequently decreasing due to bleaching. Notably, a subtle plateau occurred in the
108 curves from *M. violacea* between stimulus intensities of ~40 and 700 lux [equivalent to 1.6-2.8
109 $\log_{10}$(lux)], before continuing to increase until the response reached its peak. A closer examination of
110 the ERG waveforms themselves revealed that, in all species, the speed of the visual response (*i.e.,*
111 time taken for the b-wave to reach its peak) became faster at higher intensities (Fig. S5). Additionally,
112 the photoreceptor-derived component of the waveform (*i.e.,* a-wave amplitude) also increased at
113 higher intensities, very minimally in *O. compressus*, more substantially in *N. sammara* and greatly in
114 *M. violacea* (Fig. S5).

115 There were notable differences in the *V/logI* curves between diel period and species. The
116 *V/logI* curves were bright-shifted during the day compared to the night for *O. compressus* and *N.*
117 *sammara*, but not *M. violacea*. Furthermore, when considering the same diel period, the *V/logI* curves
118 differed between the three species, with the nature of these differences quantified using analyses of
119 the area under the curve (AUC) within the intensity ranges of bright (>10 lux), dim (<0.002 lux) or
120 overall (all intensities). Interspecific trends in the AUC values were the same irrespective of whether
121 the data was normalised to V_{max} alone or V_{max} and eye size (Fig. 3; Table S4). Firstly, regardless of
122 intensity category (*i.e.,* overall, bright, or dim), *M. violacea* had the greatest AUCs during the night,
123 followed by *N. sammara* and then *O. compressus* (Fig. 3, Table S4), indicating that the holocentrids
124 were more sensitive to both bright and dim intensities during the night than *O. compressus*. At dim
125 intensities during the day, *M. violacea* was the only species that had a calculable AUC, indicating that
126 *M. violacea* was the only species sensitive to dim intensities during the day. Finally, for both overall
127 and bright intensities, *O. compressus* had the greatest AUCs during the day, followed by *N. sammara*
128 and then *M. violacea*, indicating that *O. compressus* was more sensitive to brighter intensities during
129 the day than both holocentrids.

130

131 *Holocentrids had faster estimated retinal release kinetics compared to cardinalfish*
132 The retinal release kinetics of each species' rhodopsin protein were estimated using AA substitutions.
133 The *O. compressus* RH1 possessed four AA substitutions known to alter retinal release rate, while
134 those in *N. sammara* and *M. violacea* had six and seven AA substitutions, respectively (Table 1).
135 These substitutions resulted in reduced estimated retinal release times for the rhodopsins of all three
136 species when compared to wild-type rhodopsin. Estimations of the cumulative decrease in retinal
137 release half-life were greatest in *M. violacea* ($t_{1/2}$ difference of -6.6 min), followed by *N. sammara* (-5.3
138 min) and then *O. compressus* (-4.3 min). Therefore, the rhodopsins of both holocentrids had faster
139 estimated retinal release kinetics than that of *O. compressus*.

bioRxiv preprint doi: https://doi.org/10.1101/2022.11.27.518067; this version posted November 27, 2022. The copyright holder for this preprint (which was not certified by peer review) is the author/funder, who has granted bioRxiv a license to display the preprint in perpetuity. It is made available under aCC-BY-NC 4.0 International license.

140 **Discussion**

141 Here, we investigated the retinal structure and visual function of nocturnal reef fishes with and without
142 multibank retinas. Firstly, we confirmed that, at the morphological level, the three species investigated
143 had visual systems that were well-adapted to their dim light environments (Fig. 1; Fig. S1; Table S2).
144 In accordance with their nocturnal lifestyle (11, 12, 35), all three species had high rod densities and
145 high rod:GC summation, and low cone and GC densities. Additionally, like other holocentrid species
146 (12), *N. sammara* and *M. violacea* had multiple rod banks across the entire retina. Similar to other
147 nocturnal reef fishes (11, 12), all three species also retained some degree of photopic adaptation, with
148 cones organised into regional specialisations. However, the degree of scotopic and photopic
149 adaptations varied between the three species with *N. sammara* and *M. violacea* showing greater
150 adaptation for scotopic vision (*i.e.,* higher rod densities and summation and multibank retinas) but
151 inferior adaptation for photopic vision (*i.e.,* lower cone densities) compared to *O. compressus*.

152 Secondly, this study examined temporal resolution (or speed) of vision in these fishes by
153 determining the flicker fusion frequency (FFF) (Fig. 2; Fig. S3; Table S3). Temporal resolution is
154 fundamentally determined by the integration time of photoreceptors, with cones displaying faster
155 dynamics than rods (36). Thus, FFF is generally slower in conditions when rod responses dominate,
156 such as in species with rod-dominated retinas (*e.g.,* deep-sea fishes), at night and for lower stimulus
157 intensities (22, 32). Consequently, the maximal FFF of deeper-dwelling and nocturnal fishes ranges
158 from about 9 to 40 Hz, compared to the 40 to 100 Hz in shallow-dwelling diurnal fishes (32, 34, 37).
159 Similar to findings in other fishes (38), the FFF of *O. compressus, N. sammara,* and *M. violacea*
160 varied with diel period and stimulus intensity. All species had dim-stimulus night-time FFFs
161 comparable to other nocturnal reef fishes, however, the peak FFF (*i.e.,* elicited with bright stimuli
162 during the day) only fit within the range for other nocturnal fishes for *O. compressus* (~40 Hz) (33).
163 FFF peaked at much higher values for both *N. sammara* (70 Hz) and *M. violacea* (~60 Hz), falling
164 within a range that is usually characteristic of diurnal fishes (33, 34). The fact that *O. compressus* had
165 the highest cone and lowest rod densities but not the highest peak FFF implies that more complex
166 neuronal mechanisms are at play in the holocentrids, likely due to the structure of the multibank
167 retina. To our knowledge, the only other multibank representative whose temporal resolution has
168 been assessed was that of a deep-sea fish (*Lepidocybium flavobrunneum*) which was slow-moving
169 and had a much lower FFF [9 Hz; (22)]. It is possible that the higher temporal resolution in
170 holocentrids may represent an adaptation for active life in shallow waters (39, 40).

171 Finally, we assessed luminous sensitivity (Fig. 3; Fig. S4; Table S4). In fishes, luminous
172 sensitivity usually varies with diel period due to a dominance of cone- and rod-based responses at
173 day and night, respectively (32, 36). Our findings revealed that *N. sammara* and *O. compressus* were
174 no exception, showing higher bright-light sensitivity during the day but higher dim-light sensitivity
175 during the night. However, the sensitivity of *M. violacea* was relatively constant. This indicates that *M.*
176 *violacea* may only undergo a weak diel switch between photopic and scotopic systems. This is likely
177 due to their lack of a well-developed photopic system to switch to, similar to some deep-sea fishes
178 with pure rod retinas (41).

bioRxiv preprint doi: https://doi.org/10.1101/2022.11.27.518067; this version posted November 27, 2022. The copyright holder for this preprint (which was not certified by peer review) is the author/funder, who has granted bioRxiv a license to display the preprint in perpetuity. It is made available under aCC-BY-NC 4.0 International license.

179 Luminous sensitivity also varies with retinal structure and ecology. For example, diurnal fish
180 (with higher cone densities) have greater day-time bright-light sensitivity, while nocturnal fish (higher
181 rod densities) have greater night-time dim-light sensitivity (31, 32). Similarly, this study found
182 increasing dim-light sensitivity at night with increasing rod densities and rod banking. This supports
183 the theory that the multibank retina enhances dim-light sensitivity. Conversely, our findings showed
184 increasing bright-light sensitivity during the day with increasing cone densities, suggesting that the
185 multibank retina has less involvement in photopic vision when cones can be used instead. Finally,
186 increasing rod densities and banking (and decreasing cone densities) enhanced bright-light sensitivity
187 at night when rod responses dominate. However, it is unlikely that holocentrids need to respond to
188 any bright intensities at night. Instead, the rods in the multibank retina may be facilitating bright-light
189 sensitivity simply when the use of cones is restricted (*e.g.,* when the retina is rod-dominated in dim-
190 light specialised species). Interestingly, this rod-based bright-light sensitivity seems to be masked by
191 the higher bright-light sensitivity of the cones during the day, particularly in *N. sammara*. Notably, the
192 potentially rod-based bright-light sensitivity of the holocentrids did not seem to grant them the same
193 level of day-time bright-light sensitivity as a fish with higher cone densities. However, their level of
194 sensitivity would likely still be sufficient to meet their day-time ecological demands, such as courtship
195 and predator avoidance (42, 43). Hence, as previously proposed (44), this finding suggests that
196 holocentrids use the different layers of rods to regenerate the visual response, permitting some rod-
197 based vision under brighter intensities during the day.

198 Our study suggests that the rods in the holocentrid multibank retina can still function at
199 brighter intensities. However, rhodopsin normally bleaches at high intensities. A key reason for this
200 bleaching is the slower retinal release rate of rhodopsin compared to the cone opsins (45, 46). Amino
201 acid-based estimations of retinal release in our study species revealed that the holocentrids may have
202 accelerated retinal release kinetics compared to cardinalfishes and a wildtype reference rhodopsin,
203 which would allow their rods to recover more rapidly post-bleaching (Table 1). Supporting a faster
204 recovery rate in holocentrids, we also found higher temporal resolution at both day and night
205 compared to *O. compressus* despite their less well-developed photopic visual systems. Furthermore,
206 work in mice has shown that rods can recover and respond to bright intensities and that this is
207 facilitated by more efficient post-bleaching regeneration (47, 48). Future work using *in vitro*
208 regeneration experiments to test the retinal release kinetics of holocentrid RH1 visual pigments may
209 be used to explain how their rods continue to function at brighter intensities.

210 Overall, our findings suggest a dual role for the multibank retina, where at dim intensities it
211 functions to enhance photon capture while at bright intensities, it functions to regenerate the visual
212 response, allowing the eye to function at both lower and higher intensities than a retina with a single
213 rod bank. Enhanced visual functionality at both bright and dim light intensities aligns well with the
214 ecology of holocentrids, since they are nocturnal foragers but are still somewhat active on the reef
215 during the day (42). Our results strongly support one of the predominant theories on the function of
216 the multibank retina (16). However, it still remains possible that the multibank retina also permits

bioRxiv preprint doi: https://doi.org/10.1101/2022.11.27.518067; this version posted November 27, 2022. The copyright holder for this preprint (which was not certified by peer review) is the author/funder, who has granted bioRxiv a license to display the preprint in perpetuity. It is made available under aCC-BY-NC 4.0 International license.

217 colour vision in dim light (20). This second theory may be investigated behaviourally in future work
218 using accessible, easy-to-maintain species with multibank retinas, such as the holocentrids.

bioRxiv preprint doi: https://doi.org/10.1101/2022.11.27.518067; this version posted November 27, 2022. The copyright holder for this preprint (which was not certified by peer review) is the author/funder, who has granted bioRxiv a license to display the preprint in perpetuity. It is made available under aCC-BY-NC 4.0 International license.

219 **Materials and Methods**

220 **Animal collection and ethics.** Details of all animals are given in Table S1. Adult fish were collected from the
221 Great Barrier Reef around Lizard Island, Australia or sourced from a supplier, Cairns Marine, which also collects
222 from the northern Great Barrier Reef. All collections and procedures were conducted under a Great Barrier Reef
223 Marine Park Permit (G17/38160.1), a Queensland General Fisheries Permit (180731), and a University of
224 Queensland's Animal Ethics Permit (QBI 304/16). Following euthanasia, all animals were photographed with a
225 scale reference to quantify body length and eye diameter. Eyes were dissected and the eye cup preserved in
226 RNAlater or paraformaldehyde [PFA; 4% (w/v) PFA in 0.01M phosphate-buffered saline (PBS), pH 7.4]
227 depending on the analyses.

228

229 **Histology.** Five retinal regions (dorsal, ventral, central, nasal and temporal) were dissected, processed and
230 sectioned from PFA-fixed eyes as described in (12). The densities of key retinal cell types (*i.e.,* cones, rods, INL
231 cells and GC) per 0.01 mm^2 of retina were estimated from sections using Fiji v1.53c (49) as described elsewhere
232 [SI Appendix; (29)]. Densities were corrected for cell size using Abercrombie's correction (50) (Fig. 1).

233

234 **Electroretinography (ERG).** Corneal ERG recordings were conducted *in vivo* on whole, intact eyes to assess
235 visual function using methods similar to those described in (33). Fish were acclimatised to the recording chamber
236 for 30 min, anaesthetised with 0.2 mL clove oil/litre seawater, immobilised with an intramuscular injection of 8.5
237 mg/kg gallamine triethiodide and ventilated with oxygenated seawater (Fig. S2). After ≥40 min of dark adaptation,
238 light stimuli were delivered to the eye using a custom-built, calibrated, broad-spectrum light source controlled via
239 a PowerLab 4/26 DAQ module. Visual responses were detected through silver wire electrodes placed on the
240 surface of the eye, amplified via a DP-103 amplifier and acquired in LabChart 8 v8.1.16. The system was
241 grounded to the water of the recording chamber. Recordings were conducted at 28 ± 1˚C at both day and night to
242 control for any effects of temperature and circadian rhythm, respectively. Recordings were performed at the
243 Lizard Island Research Station (LIRS) or the Queensland Brain Institute (QBI). Additional recordings were taken
244 at both sites to compare results between the recording locations (Fig. S6).

245

246 **Temporal resolution ERGs.** The temporal resolution of vision was assessed using flicker fusion frequency (FFF)
247 ERGs. FFF is the point at which evenly spaced light pulses can no longer be distinguished as separate. Dark-
248 adapted FFF ERGs were recorded by increasing the frequency of white light stimuli of constant intensity from 5
249 Hz to 95 Hz at increments of 5 Hz. Light pulses were 10 ms in duration and were repeated 30 times. Recordings
250 were conducted for bright (384 lux) and dim (4 lux) stimuli (Fig. 2). The FFF threshold was determined either
251 through visual inspection (at lower frequencies, <65 Hz) or by using the power spectrum to differentiate the signal
252 and noise (at higher frequencies, ≥65 Hz) [SI Appendix; (34, 51)]. Statistics and graphs throughout the study
253 were generated in GraphPad Prism v9.0.0.

254

255 **Absolute sensitivity ERGs.** The absolute (luminous) sensitivity of vision was determined using *V/logI* curves,
256 which plot the normalised amplitude of the response, *V* (Fig. S2), against the log of the intensity (*I*). These ERGs
257 were recorded by increasing the intensity of a white light from 2.4×10^{-8} to 240,000 lux [*i.e.,* -7.6 to 5.4 $\log_{10}$(lux)] in
258 0.3-0.6 log unit steps. Light stimuli were 100 ms pulses presented at 0.1 – 0.4 Hz (SI Appendix) and were
259 repeated ten times for each intensity. The mean response amplitudes were normalised to the maximal response
260 (V_{max}) and plotted against stimulus intensity to obtain the *V/logI* curve (33, 52). The area under the curve (AUC)
261 was calculated as a proxy for the magnitude and breadth of the visual responses. AUC was calculated for either
262 all intensities, dim intensities (<0.002 lux) or bright intensities (>10 lux) for each species (Fig. 3). To isolate the
263 effect of the multibank retina, the V_{max}-normalised responses were also normalised to eye size (to obtain
264 responses per unit of retina) and analysed again as described above. To further understand how the visual
265 response changed with intensity, representative ERG waveforms were analysed to obtain: 1) the time from
266 stimulus presentation to the peak of the signal generated post-synaptic to the photoreceptors (*i.e.,* time to b-wave
267 peak; ms) and 2) the amplitude of the photoreceptor-derived peak (*i.e,* a-wave amplitude; mV). These values
268 were obtained for dim (0.4 lux), moderate (125 lux) and bright (2165 lux for *O. compressus* and 5160 lux for *N.*
269 *sammara* and *M. violacea*) stimuli, which matched the base, peak and decline of the *V/logI* curves, respectively.

270

271 **Estimations of retinal release kinetics.** Amino acid substitution sites involved in retinal release kinetics were
272 used to estimate the retinal release time of the rhodopsin protein in each species (Table 1). Firstly, 12 candidate
273 amino acid (AA) substitution sites were identified from the literature (53-55). Notably, retinal release effect has
274 not been characterised for all positively selected non-spectral substitutions in the literature (*e.g.,* T97S in *N.*
275 *sammara* and F116S and A164G in *M. violacea*) and that any substitutions that also affected spectral sensitivity
276 were excluded from these analyses. Next, the rhodopsin coding sequences for *O. compressus* (MH979489.1), *N.*

bioRxiv preprint doi: https://doi.org/10.1101/2022.11.27.518067; this version posted November 27, 2022. The copyright holder for this preprint (which was not certified by peer review) is the author/funder, who has granted bioRxiv a license to display the preprint in perpetuity. It is made available under aCC-BY-NC 4.0 International license.

277 *sammara* (MW219675.1) and *M. violacea* (MW219672.1) (11, 12) were downloaded from GenBank
278 (https://www.ncbi.nlm.nih.gov/genbank/) and translated to protein sequences. These were manually inspected for
279 AA substitutions at each of the 12 candidate sites in Geneious Prime v2021.1.1. Identified substitutions were
280 used to estimate the cumulative change in retinal release, calculated as the difference in retinal release half-life
281 ($t_{1/2}$; min) compared to wild-type zebrafish (53), bovine (55) or catfish (56) rhodopsin, depending on the study
282 (Table 1).

283

284

285 **Funding.** This research was supported by an Australian Research Council (ARC) DECRA awarded to FdB
286 (DE180100949) and the Queensland Brain Institute. Furthermore, FC was supported by an ARC DECRA
287 (DE200100620) and NJM by an ARC Laureate Fellowship (FL140100197). LF was supported by an Australian
288 Government Research Training Program Stipend and a Queensland Brain Institute Research Higher Degree Top
289 Up Scholarship.

290 **Acknowledgements.** We acknowledge the Dingaal, Ngurrumungu and Thanhil peoples as traditional owners of
291 the lands and waters of the Lizard Island region from where specimens were collected. We also acknowledge the
292 traditional owners of the land on which the University of Queensland is situated, the Turrbal/Jagera people. We
293 would like to thank Cairns Marine for supplying animals and the staff at Lizard Island Research Station, Anne
294 Hoggett and Lyle Vail, for support during field work. We thank Robert Sullivan from the Queensland Brain
295 Institute (QBI) Histology Facility, Richard Webb and Robyn Chapman Webb from the Centre for Microscopy and
296 Microanalysis (CMM) and Rumelo Amor from the QBI Advanced Microscopy facility for technical support and
297 advice. Finally, we thank Dr Martin Luehrmann for invaluable guidance and discussions about the findings.

298 **Data Availability.** All study data are included in the article and/or SI Appendix.

bioRxiv preprint doi: https://doi.org/10.1101/2022.11.27.518067; this version posted November 27, 2022. The copyright holder for this preprint (which was not certified by peer review) is the author/funder, who has granted bioRxiv a license to display the preprint in perpetuity. It is made available under aCC-BY-NC 4.0 International license.

299 **References**

300 1. H. H. Thoen, M. J. How, T.-H. Chiou, J. Marshall, A Different Form of Color Vision in Mantis Shrimp. *Science* **343**, 411-413 (2014).
301 2. H. G. Krapp, Polarization Vision: How Insects Find Their Way by Watching the Sky. *Current Biology* **17**, R557-R560 (2007).
302 3. R. K. Schott *et al.*, Evolutionary transformation of rod photoreceptors in the all-cone retina of a diurnal garter snake. *Proceedings of the National Academy of*
303 *Sciences of the United States of America* **113**, 356-361 (2016).
304 4. N. Bhattacharyya, B. Darren, R. K. Schott, V. Tropepe, B. S. W. Chang, Cone-like rhodopsin expressed in the all-cone retina of the colubrid pine snake as a
305 potential adaptation to diurnality. *The Journal of experimental biology* **220**, 2418-2425 (2017).
306 5. L. S. V. Roth, A. Kelber, *Nocturnal colour vision in geckos* (2005), vol. 271 Suppl 6, pp. S485-487.
307 6. J. E. Cohen, J. R. Beddington, D. H. Cushing, R. M. May, J. H. Steele, Marine and continental food webs: three paradoxes? *Philosophical Transactions of*
308 *the Royal Society of London. Series B: Biological Sciences* **343**, 57-69 (1994).
309 7. F. de Busserolles, L. Fogg, F. Cortesi, J. Marshall, The exceptional diversity of visual adaptations in deep-sea teleost fishes. *Seminars in Cell &*
310 *Developmental Biology* **106**, 20-30 (2020).
311 8. F. Cortesi *et al.*, Visual system diversity in coral reef fishes. *Seminars in Cell & Developmental Biology* **106**, 31-42 (2020).
312 9. L. Schmitz, P. C. Wainwright, Nocturnality constrains morphological and functional diversity in the eyes of reef fishes. *BMC Evolutionary Biology* **11**, 338
313 (2011).
314 10. S. P. Collin, R. V. Hoskins, J. C. Partridge, Tubular Eyes of Deep-Sea Fishes: A Comparative Study of Retinal Topography (Part 1 of 2). *Brain, behavior and*
315 *evolution* **50**, 335-346 (1997).
316 11. M. Luehrmann, K. L. Carleton, F. Cortesi, K. L. Cheney, N. J. Marshall, Cardinalfishes (Apogonidae) show visual system adaptations typical of nocturnally
317 and diurnally active fish. *Molecular ecology* **28**, 3025-3041 (2019).
318 12. F. de Busserolles *et al.*, The visual ecology of Holocentridae, a nocturnal coral reef fish family with a deep-sea-like multibank retina. *The Journal of*
319 *experimental biology* **224**, jeb233098 (2021).
320 13. N. W. Pankhurst, The relationship of ocular morphology to feeding modes and activity periods in shallow marine teleosts from New Zealand. *Environmental*
321 *Biology of Fishes* **26**, 201-211 (1989).
322 14. J. Shand (1994) Changes in the visual system of teleost fishes during growth and settlement: an ecological perspective. in *Department of Marine Biology*
323 (James Cook University), p 260.
324 15. W. N. McFarland, "The Visual World of Coral Reef Fishes" in The Ecology of Fishes on Coral Reefs*,* P. F. Sale, Ed. (Academic Press, Inc., San Diego,
325 California, 1991), pp. 16-36.
326 16. H. J. Wagner, E. Frohlich, K. Negishi, S. P. Collin, The eyes of deep-sea fish. II. Functional morphology of the retina. *Progress in retinal and eye research*
327 **17**, 637-685 (1998).
328 17. N. A. Locket, The multiple bank rod fovea of *Bajacalifornia drakei*, an alepocephalid deep-sea teleost. *Proceedings of the Royal Society of London. Series B.*
329 *Biological Sciences* **224**, 7-22 (1985).
330 18. K. Awaiwanont, W. Gunarso, M. Sameshima, S. Hayashi, G. Kawamura, Grouped, stacked rods and tapeta lucida in the retina of Japanese anchovy
331 *Engraulis japonicus*. *Fisheries Science* **67**, 804-810 (2001).
332 19. E. Frohlich, H. J. Wagner, Development of multibank rod retinae in deep-sea fishes. *Visual neuroscience* **15**, 477-483 (1998).
333 20. E. J. Denton, N. A. Locket, Possible Wavelength Discrimination by Multibank Retinae in Deep-Sea Fishes. *Journal of the Marine Biological Association of*
334 *the United Kingdom* **69**, 409-435 (1989).
335 21. V. B. Meyer-Rochow, P. A. Coddington, "Eyes and Vision of the New Zealand Torrentfish *Cheimarrichthys fosterae* Von Haast (1874): Histology,
336 Photochemistry and Electrophysiology" in Fish Adaptations*,* V. A.L., K. B.G, Eds. (Oxford and IBH Publ. & M/s Sci. Publ., Enfield, New Hampshire & Plymouth, 2003),
337 chap. 15, pp. 337-383.
338 22. E. Landgren, K. Fritsches, R. Brill, E. Warrant, The visual ecology of a deep-sea fish, the escolar *Lepidocybium flavobrunneum* (Smith, 1843). *Philosophical*
339 *transactions of the Royal Society of London. Series B, Biological sciences* **369**, 20130039-20130039 (2014).
340 23. R. Shapley, J. Gordon, The visual sensitivity of the retina of the conger eel. *Proceedings of the Royal Society of London. Series B. Biological Sciences* **209**,
341 317-330 (1980).
342 24. M. M. Hess, R.R.; Smola U. , The photoreceptors of *Muraena helena* and *Ariosoma balearicum* - a comparison of multiple bank retinae in anguilliform eels
343 (Teleostei). *Zoologischer Anzeiger* **237**, 127-137 (1998).
344 25. J. S. Nelson, *Fishes of the world* (John Wiley & Sons, Inc., New York, ed. 3rd, 1994).
345 26. D. W. Greenfield, J. E. Randall, P. N. Psomadakis, A review of the soldierfish genus *Ostichthys* (Beryciformes: Holocentridae), with descriptions of two new
346 species from Myanmar. *Journal of the Ocean Science Foundation* **26**, 1-33 (2017).
347 27. M. H. Horn, L.M. Karen and M.A. Chotkowski, *Intertidal fishes: life in two worlds* (Academic Press, USA, 1999), pp. 399.
348 28. L. G. Fogg *et al.*, Development of dim-light vision in the nocturnal reef fish family Holocentridae I: Retinal gene expression. *Journal of Experimental Biology*
349 **225**, jeb244513 (2022).
350 29. L. G. Fogg *et al.*, Development of dim-light vision in the nocturnal reef fish family Holocentridae II: Retinal morphology *Journal of Experimental Biology* **225**,
351 jeb244740 (2022).
352 30. W. Toller (1996) Rhodopsin Evolution in the Holocentridae (Pisces: Beryciformes). in *Faculty of the Graduate School* (University of Southern California).
353 31. H. Kobayashi, A comparative study on electroretinogram in fish, with special reference to ecological aspects. *Shimonoseki College of Fisheries* **353**, 407-
354 538 (1962).
355 32. M. A. Ali, *Vision in Fishes: New Approaches in Research* (Plenum Publishing Corporation, New York and London, 1975), vol. 1, pp. 824.
356 33. A. Z. Horodysky, R. W. Brill, E. J. Warrant, J. A. Musick, R. J. Latour, Comparative visual function in five sciaenid fishes inhabiting Chesapeake Bay. *Journal*
357 *of Experimental Biology* **211**, 3601 (2008).
358 34. W. S. Chung, N. J. Marshall, S. A. Watson, P. L. Munday, G. E. Nilsson, Ocean acidification slows retinal function in a damselfish through interference with
359 GABAA receptors. *The Journal of experimental biology* **217**, 323-326 (2014).
360 35. L. Fishelson, G. Ayalon, A. Zverdling, R. Holzman, Comparative morphology of the eye (with particular attention to the retina) in various species of cardinal
361 fish (Apogonidae, Teleostei). *The anatomical record. Part A, Discoveries in molecular, cellular, and evolutionary biology* **277**, 249-261 (2004).
362 36. I. Perlman, "The Electroretinogram: ERG" in Webvision: The Organization of the Retina and Visual System*,* F. E. Kolb H, Nelson R, Ed. (University of Utah
363 Health Sciences Center, Salt Lake City, 2001).
364 37. A. Z. Horodysky, R. W. Brill, K. C. Crawford, E. S. Seagroves, A. K. Johnson, Comparative visual ecophysiology of mid-Atlantic temperate reef fishes.
365 *Biology Open* **2**, 1371 (2013).
366 38. A. Z. Horodysky, R. W. Brill, E. J. Warrant, J. A. Musick, R. J. Latour, Comparative visual function in four piscivorous fishes inhabiting Chesapeake Bay. *The*
367 *Journal of experimental biology* **213**, 1751-1761 (2010).
368 39. W. B. Gladfelter, W. S. Johnson, Feeding Niche Separation in a Guild of Tropical Reef Fishes (Holocentridae). *Ecology* **64**, 552-563 (1983).
369 40. D. W. Greenfield, "Holocentridae: squirrelfishes (soldierfishes)" in The living marine resources of the Western Central Atlantic*,* K. E. Carpenter, Ed. (Food
370 and Agriculture Organization of the United Nations, Rome, Italy, 2002), vol. 5, pp. 1192-1202.
371 41. J. H. S. Blaxter, M. Staines, Pure-Cone Retinae and Retinomotor Responses in Larval Teleosts. *Journal of the Marine Biological Association of the United*
372 *Kingdom* **50**, 449-464 (1970).
373 42. H. Winn, J. A. Marshall, B. Hazlett, Behavior, Diel Activities, and Stimuli that Elicit Sound Production and Reactions to Sounds in the Longspine Squirrelfish.
374 *Copeia* **1964**, 413-425 (1964).
375 43. B. A. Carlson, A. H. Bass, Sonic/Vocal Motor Pathways in Squirrelfish (Teleostei, Holocentridae). *Brain, behavior and evolution* **56**, 14-28 (2000).
376 44. E. Frohlich, H.-J. Wagner, Rod Outer Segment Renewal in the Retinae of Deep-sea Fish. *Vision research* **36**, 3183-3194 (1996).
377 45. M.-H. Chen, C. Kuemmel, R. R. Birge, B. E. Knox, Rapid Release of Retinal from a Cone Visual Pigment following Photoactivation. *Biochemistry* **51**, 4117-
378 4125 (2012).
379 46. N. T. Ingram, A. P. Sampath, G. L. Fain, Why are rods more sensitive than cones? *The Journal of physiology* **594**, 5415-5426 (2016).
380 47. A. Kelber, Vision: Rods See in Bright Light. *Current Biology* **28**, R364-R366 (2018).
381 48. A. Tikidji-Hamburyan *et al.*, Rods progressively escape saturation to drive visual responses in daylight conditions. *Nature Communications* **8**, 1813 (2017).
382 49. J. Schindelin *et al.*, Fiji: an open-source platform for biological-image analysis. *Nature Methods* **9**, 676 (2012).
383 50. M. Abercrombie, Estimation of nuclear population from microtome sections. *The Anatomical Record* **94**, 239-247 (1946).
384 51. K. A. Fritsches, R. W. Brill, E. J. Warrant, Warm eyes provide superior vision in swordfishes. *Current biology : CB* **15**, 55-58 (2005).
385 52. T. M. Frank, Effects of Light Adaptation on the Temporal Resolution of Deep-sea Crustaceans. *Integr Comp Biol* **43**, 559-570 (2003).
386 53. J. M. Morrow, B. S. W. Chang, Comparative Mutagenesis Studies of Retinal Release in Light-Activated Zebrafish Rhodopsin Using Fluorescence
387 Spectroscopy. *Biochemistry* **54**, 4507-4518 (2015).
388 54. G. M. Castiglione, R. K. Schott, F. E. Hauser, B. S. W. Chang, Convergent selection pressures drive the evolution of rhodopsin kinetics at high altitudes via
389 nonparallel mechanisms. *Evolution* **72**, 170-186 (2017).
390 55. F. E. Hauser *et al.*, Accelerated Evolution and Functional Divergence of the Dim Light Visual Pigment Accompanies Cichlid Colonization of Central America.
391 *Molecular biology and evolution* **34**, 2650-2664 (2017).
392 56. G. M. Castiglione *et al.*, Evolution of nonspectral rhodopsin function at high altitudes. *Proceedings of the National Academy of Sciences of the United States*
393 *of America* **114**, 7385-7390 (2017).

394
395

bioRxiv preprint doi: https://doi.org/10.1101/2022.11.27.518067; this version posted November 27, 2022. The copyright holder for this preprint (which was not certified by peer review) is the author/funder, who has granted bioRxiv a license to display the preprint in perpetuity. It is made available under aCC-BY-NC 4.0 International license.

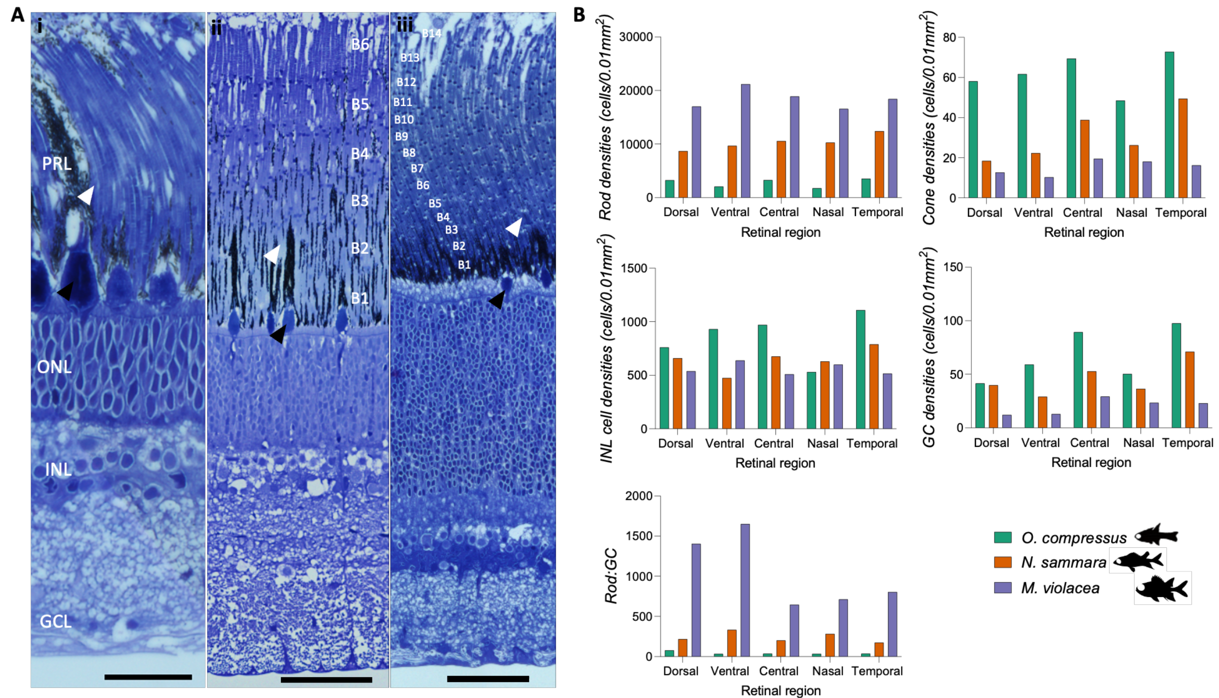

396

397 *Fig. 1. Retinal structure and cell densities.* **A**. Representative radial sections from the retina of **i**) *O.*
398 *compressus*, **ii**) *N. sammara* and **iii**) *M. violacea*. Rod banks are numbered as B_n. Representative rod
399 and cone outer segments are indicated by black and white arrows, respectively. **B**. Densities of
400 different types of retinal cells in *O. compressus* (*n*=1), *N. sammara* (*n*=1) and *M. violacea* (*n*=1). PRL,
401 photoreceptor layer; ONL, outer nuclear layer; INL, inner nuclear layer; GCL, ganglion cell layer; GC,
402 ganglion cells. Scale bars: 25 μm (Ai), 50 μm (Aii and Aiii).

403

bioRxiv preprint doi: https://doi.org/10.1101/2022.11.27.518067; this version posted November 27, 2022. The copyright holder for this preprint (which was not certified by peer review) is the author/funder, who has granted bioRxiv a license to display the preprint in perpetuity. It is made available under aCC-BY-NC 4.0 International license.

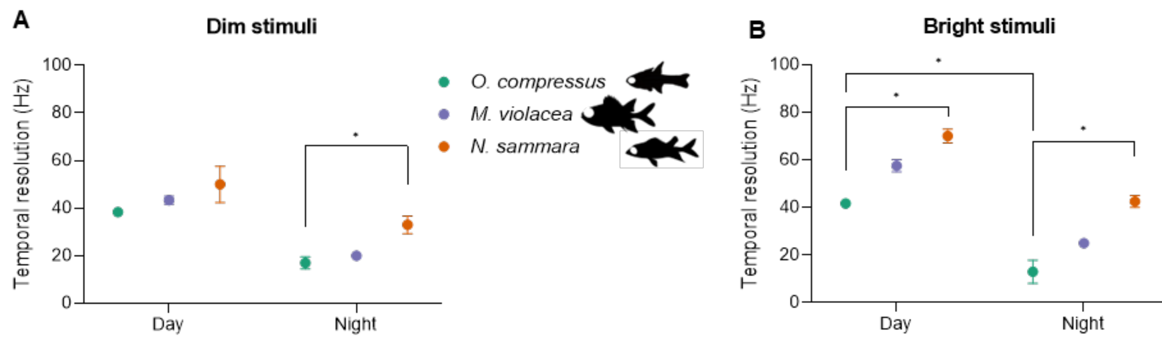

404

405 *Fig. 2. Temporal resolution electroretinography (ERG).* ERG waveforms were obtained for a range of
406 stimulus frequencies from 5 to 95 Hz. The temporal correlation of resultant waveforms with the
407 stimulus were used to derive the maximal temporal resolution (*i.e.,* flicker fusion frequency) elicited
408 using either **A**) dim (4 lux) or **B**) bright (384 lux) stimuli in *O. compressus* (*n*=3 and 5 for day and night
409 recordings, respectively), *N. sammara* (*n*=3 and 5 for day and night recordings, respectively) and *M.*
410 *violacea* (*n*=3 and 5 for day and night recordings, respectively). Data represent mean ± s.e.m.
411 Statistical significance (calculated from a Kruskal-Wallis with Dunn's multiple comparisons test): *,
412 p<0.05.
413

bioRxiv preprint doi: https://doi.org/10.1101/2022.11.27.518067; this version posted November 27, 2022. The copyright holder for this preprint (which was not certified by peer review) is the author/funder, who has granted bioRxiv a license to display the preprint in perpetuity. It is made available under aCC-BY-NC 4.0 International license.

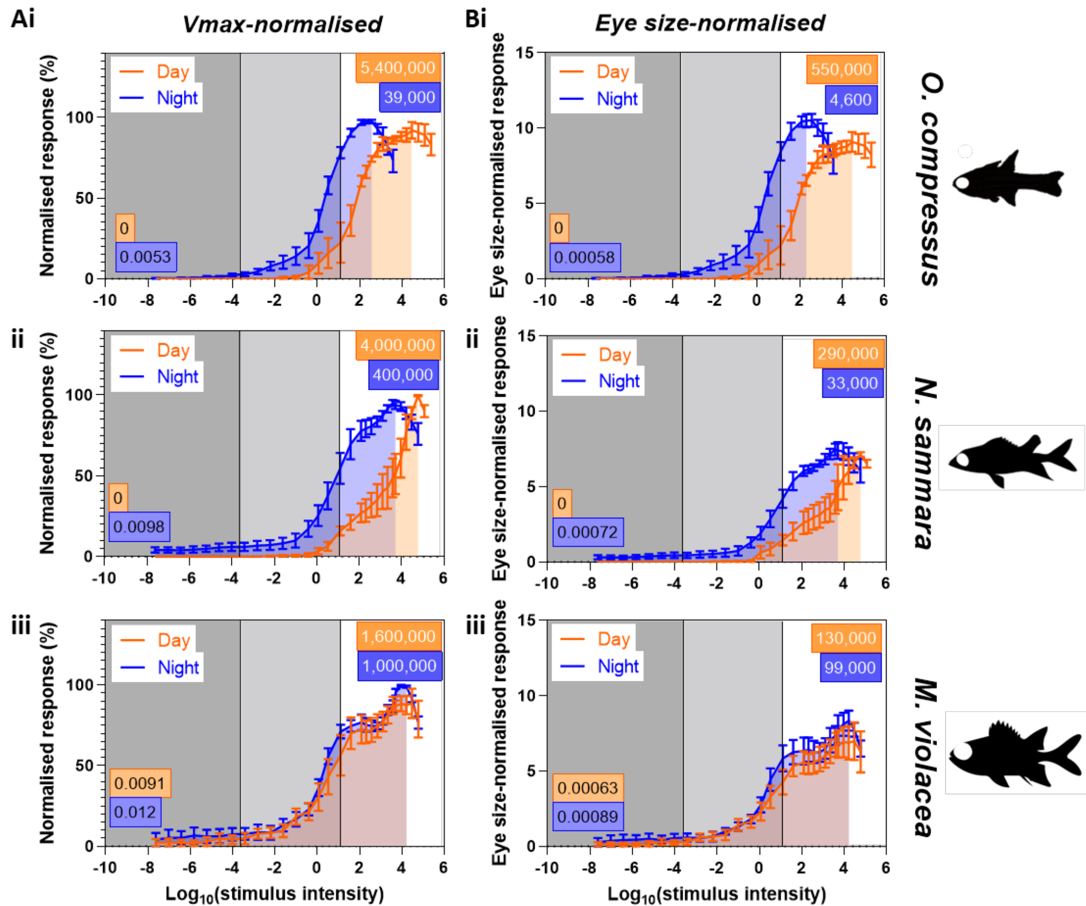

414

415 *Fig. 3. V/logI curves from absolute sensitivity electroretinography (ERG).* ERG waveforms were
416 obtained for a range of intensities from 2.4×10^{-8} to 240,000 lux [*i.e.,* -7.6 to 5.4 $\log_{10}$(lux)] and the
417 mean b-wave amplitude from each set of waveforms was plotted against the $\log_{10}$ of the stimulus
418 intensity (in lux) normalised to either **A**) the maximal response (V_{max}; response given as % of V_{max}) or
419 **B**) both V_{max} and eye size for **i**) *O. compressus* (*n*=5), **ii**) *N. sammara* (*n*=4 and 5 for day and night
420 recordings, respectively), and **iii**) *M. violacea* (*n*=4) at day (orange) and night (blue). Each graph is
421 divided into bright (white; >10 lux), intermediate (light grey; 0.002-10 lux) and dim (dark grey; <0.002
422 lux) intensities. Shaded regions under the line graphs represent the total area under the curve (AUC)
423 from the lowest detectable response up to the maximal response. Values in the coloured boxes
424 represent the rounded AUC values for dim (black text; bottom left) or bright intensities (white text; top
425 right). Data are mean ± s.e.m.
426

bioRxiv preprint doi: https://doi.org/10.1101/2022.11.27.518067; this version posted November 27, 2022. The copyright holder for this preprint (which was not certified by peer review) is the author/funder, who has granted bioRxiv a license to display the preprint in perpetuity. It is made available under aCC-BY-NC 4.0 International license.

427 *Table 1. Amino acid substitutions in nocturnal reef fishes linked to retinal release kinetics.* Different
428 amino acid substitutions (AA) in teleosts that have been found to have little effect on spectral tuning
429 but alter retinal release kinetics (53-55) were examined in *O. compressus, N. sammara* and *M.*
430 *violacea*. Each candidate AA substitution is given in the first column, and the corresponding AA found
431 in the study species is given for each site. Substituted sites in the study species are in bold. The
432 influence on retinal release was defined as the difference in retinal release $t_{1/2}$ (min) compared to wild-
433 type rhodopsin.

AA substitution	***O. compressus***	***N. sammara***	***M. violacea***	**Influence on retinal release**
I209V	T	F	**V**	-1.3
F213I	M	M	L	+1.5
V266L	C	**L**	**L**	+1.7
L290I	**I**	**I**	**I**	-1.3
V286I	V	L	L	-0.9
M123I	**I**	**I**	**I**	+4.9
G124A	**A**	S	G	+1.8
C165L	C	**L**	**L**	-0.9
V189I	**I**	**I**	**I**	+2.5
L59Q	L	L	L	-6.3
Y74F	Y	Y	Y	-1.9
N83D	**D**	**D**	**D**	-12.2
Cumulative change	-4.3	-5.3	-6.6	

434